Supplemental data for

PATAS, a first-in-class therapeutic peptide biologic, improves whole-body insulin resistance and associated comorbidities *in vivo*

This file includes:

- Supplemental Research Design and Methods
- Supplemental Table
- Supplemental Figures S1-6 and Legends
- Supplemental References

SUPPLEMENTAL RESEARCH DESIGN AND METHODS

In vivo measurement of glucose uptake using 2-NBDG in the adipose tissue

2-NBDG 2-Deoxy-2-[(7-nitro-2,1,3-benzoxadiazol-4-yl)amino]-D-glucose. Sigma-Aldrich 72987. Injection buffer used with 2-NBDG was saline solution (vehicle). Dissolve 2-NBDG in PBS at 5 mM (1.71 mg/mL) and inject via the tail vein 100 uL 10 mM 2-NBDG. In parallel, 2 mg/kg pf PATAS was subcutaneously injected to the db/db BKS mice. Thirty minutes later mice were sacrificed and the visceral adipose tissue was harvested tissues for fluorescent measurements per gram of tissue. One gram of adipose tissue per mouse was then sonicated in 2 mL of lysis buffer (1 % sodium deoxycholate, 40 mM KCl, and 20 mM Tris [pH 7.4]) for 5 minutes. The tissue lysate solution was then centrifuged at 12,000 g for 10 minutes at 4°C. Fifty µL of aliquots from the supernatants were used for fluorescent measurement as described previously (PMID: 21510766). The intra adipose tissue 2-NBDG concentration ($[2\text{-NBDG}]_i$) was determined based on standard curves generated by measuring fluorescence levels of 2.5–20 mM 2-NBDG in lysis buffer.

Adipocyte analysis and primary cell culture

Adipocyte cells were isolated from adipose tissue and processed as described in Carswell et al. (1).

Adipocyte images were obtained at ×40 magnification, and morphological analyses were performed with use of Adiposoft software (Center for Applied Medical Research, University of Navarra). Adipocyte size and number were measured in two fields of 1,000 × 1,000 µm using a validated, optimized sequence of image analysis steps in Adiposoft. On average 200 adipocytes were measured per mouse with n = 5 mice per group.

Circular dichroism

For circular dichroism experiments, the PATAS peptide was dissolved in a solution containing 75 % Methanol and 25 % saline aqueous solution (0.9 %) for a final concentration of 1 mg/mL. These experiments were recorded at 25.0 ± 0.1 °C on a Jasco J-815 spectropolarimeter with 0.1 mm path-length

quartz-Suprasil cells (JASCO Inc., Easton, MD). Acquisition parameters as continuous scan rate, response time, and bandwidth were 50 nm/min, 1.0 s, and 1 nm, respectively. Data were collected in the 180−270 nm range and averaged over three successive scans.

Nuclear Magnetic Resonance

Samples were obtained by dissolving 2 mg of dry PATAS peptide powder into 170 µL of a solution containing 75 % d4-Methanol and 25 % saline aqueous solution (0.9 %). Spectra were recorded on a Bruker Avance III 700 MHz spectrometer equiped with a TCI cryoprobe. Resonance assignments were obtained from NOESY, TOCSY and 1H-13C HSQC spectra recorded at 300K using standard sequential assignment procedure. The PATAS helical structure was assessed from the observation of Hα(i)-HN(i+3) magnetization transfer (NOE) in NOESY spectra (150 ms mixing time) recorded at 283K. 3D models of PATAS in helical conformation were obtained using XPLOR-NIH software after addition of a 2-(4-octenyl) alanine in the topology library.

Quantitative nuclear magnetic resonance body mass composition determination

This series of experiments were carried out at the mouse clinic institute (ICS). Briefly, the DIO mice were caged individually over the whole period of study and were monitored daily and body weight was taken every two days. Body mass composition was determined by Quantitative Nuclear Magentic Resonance (qNMR) using the Minispec + analyzer from Bruker Biospin SAS, Wissembourg, France. The initial body mass composition was determined before PATAS treatment was initiated i.e. at D-4 and then at the end of the PATAS treatment phase i.e. D22. n = 8 mice per group.

PATAS off-target screening with SAFETYscan™ E/IC50 ELECT

PATAS was tested by independent CRO Eurofins Pharma Discovery services, Eurofins DiscoverX Corporation 11180 Roselle Street, Suite D San Diego, CA 92121 for off-target activity following their standard procedure.

Inflammation score

Hepatic inflammation score was calculated according to the criteria of Kleiner et al. (2).

PATAS pharmacokinetic study in mice

A pharmacokinetic (PK) study was performed in male ICR mice following PATAS administration (100 μg/mouse; 30 μL/mouse) at subcutaneous AT tissue (inguinal area). The serum was collected at 10 min, 30 min, 1, 2, 4, 6, 8, and 24 hours after treatment. The exposure levels of PATAS in serum samples determined by LC-MS/MS. The non-compartmental analysis (NCA) of the serum data were analyzed by using WinNonlin. For the bioanalytical method, the peptide (VECTT-R8-EKEVLA-S5-LDKAAFLTQLHS) was dissolved in 0.9 % NaCl at 3.33 mg/mL for subcutaneous AT injection. The dosing volume was set at 30 μL/mouse. Male ICR mice weighing 35 - 40 g were provided by BioLasco Taiwan (under Charles River Laboratories Licensee). Animals were acclimated for 3 days prior to use and were confirmed with good health. All animals were maintained in a hygienic environment with controlled temperature (20 - 24ºC), humidity (30 % - 70 %) and 12 hours light/dark cycles. Free access to sterilized standard lab diet [MFG (Oriental Yeast Co., Ltd., Japan)] and autoclaved tap water were granted. All aspects of this work, including housing, experimentation, and disposal of animals were performed in general accordance with the Guide for the Care and Use of Laboratory Animals: Eighth Edition (National Academy Press, Washington, D. C., 2011) in an AAALAC-accredited laboratory animal facility. The animal care and use protocol was reviewed and approved by the IACUC at Pharmacology Discovery Services Taiwan, Ltd.

SUPPLEMENTAL TABLE

TableS1: List of quantitative real-time PCR primers and probes used in this study

Gene name	**Primer sequence**	**Manufacturer**
ChREBPα	AGTGCTTGAGCCTGGCCTAC	Sigma-Aldrich
	TTGTTCAGGCGGATCTTGTC	Sigma-Aldrich
ChREBPβ	AGCGGATTCCAGGTGAGG	Sigma-Aldrich
	TTGTTCAGGCGGATCTTGTC	Sigma-Aldrich
Gene name	**Catalog #**	**Manufacturer**
FAS	Hs00236330_m1	LifeTech
ACC	Hs01046047_m1	LifeTech
SREBP1	Hs01088691_m1	LifeTech
GAPDH	4310884E-0708037	LifeTech

SUPPLEMENTAL FIGURES AND LEGENDS

Supplemental Figure S1.

A

Native peptide	Sequence	Stapling type	Stapled position
1	KDVVIQ	i; i+5	K and Q
2	ECTMVEKKVLALL	i; i+7	M and A
3	DLMYHIQQVV	i; i+5	M and Q
4	EGQAVFYAAEISIG	i; i+5	Y and S
5	SVEWWAYGLLYEMLA	i; i+5	G and M
6	EDDDELFNSIME	i; i+7	E and M
7	LSKEAVSVCK	i; i+5	S and S
8	LVEKRVL	i; i+3	V and R
9	KPSDKD	i; i+3	P and K

B

```
         10         20         30         40         50
MADVFPGNDS TASQDVANRF ARKGALRQKN VHEVKDHKFI ARFFKQPTFC
         60         70         80         90        100
SHCTDFIWGF GKQGFQCQVC CFVVHKRCHE FVTFSCPGAD KGPDTDDPRS
        110        120        130        140        150
KHKFKIHTYG SPTFCDHCGS LLYGLIHQGM KCDTCDMNVH KQCVINVPSL
        160        170        180        190        200
CGMDHTEKRG RIYLKAEVAD EKLHVTVRDA KNLIPMDPNG LSDPYVKLKL
        210        220        230        240        250
IPDPKNESKQ KTKTIRSTLN PQWNESFTFK LKPSDKDRRL SVEIWDWDRT
        260        270        280        290        300
TRNDFMGSLS FGVSELMKMP ASGWYKLLNQ EEGEYYNVPI PEGDEEGNME
        310        320        330        340        350
LRQKFEKAKL GPAGNKVISP SEDRKQPSNN LDRVKLTDFN FLMVLGKGSF
        360        370        380        390        400
GKVMLADRKG TEELYAIKIL KKDVVIQDDD VECTMVEKRV LALLDKPPFL
        410        420        430        440        450
TQLHSCFQTV DRLYFVMEYV NGGDLMYHIQ QVGKFKEPQA VFYAAEISIG
        460        470        480        490        500
LFFLHKRGII YRDLKLDNVM LDSEGHIKIA DFGMCKEHMM DGVTTRTFCG
        510        520        530        540        550
TPDYIAPEII AYQPYGKSVD WWAYGVLLYE MLAGQPPFDG EDEDELFQSI
        560        570        580        590        600
MEHNVSYPKS LSKEAVSVCK GLMTKHPAKR LGCGPEGERD VREHAFFRRI
        610        620        630        640        650
DWEKLENREI QPPFKPKVCG KGAENFDKFF TRGQPVLTPP DQLVIANIDQ
        660        670
SDFEGFSYVN PQFVHPILQS AV
```

C1 domain

C2 domain

Ca^{2+} binding domain

ATP binding domain: GxGxxG

Kinase domain

Invariant Lysine

Sequence used for stapled peptide

Gatekeeper residue

Invariant Threonine, activation loop

C Input control for Figure 1G

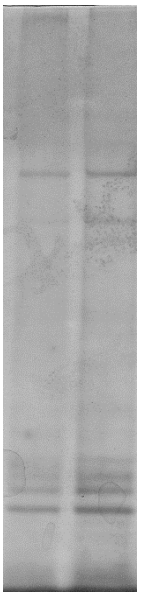

D

```
aPKC_human                KGIFGKGMLSHKKGTKEMYAIKILKKDVVIQDDDVECTMVEKRVLALLDKPPFLTQLHSC
aPKC_NHP_is_predicted     KGSFGKVMLADRKGTEELYAIKILKKDVVIQDDDVECTMVEKRVLALLDKPPFLTQLHSC
aPKC_dog                  KGSFGKVMLADRKGTEELYAIKILKKDVVIQDDDVECTMVEKRVLALLDKPPFLTQLHSC
aPKC_rat                  KGSFGKVMLADRKGTEELYAIKILKKDVVIQDDDVECTMVEKRVLALLDKPPFLTQLHSC
aPKC_mouse                KGSFGKVMLADRKGTEELYAIKILKKDVVIQDDDVECTMVEKRVLALLDKPPFLTQLHSC
```

E

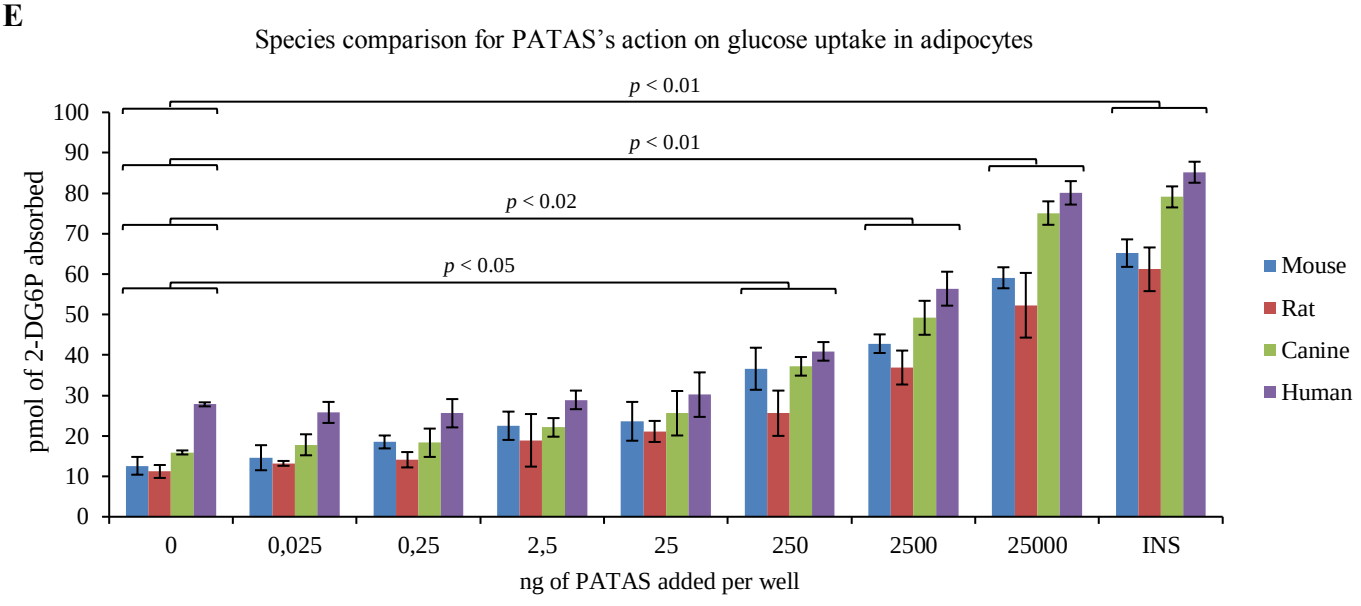

Figure S1. Identifying a unique sequence to trigger glucose absorption in the human adipocytes

(**A**) List of stapled peptides derived from identified alpha helices with their stapling type.

(**B**) Human PKC alpha primary amino sequence with identified domains, key residues (3) and the peptide sequence used for the stapled peptide (in red).

(**C**) Protein input control for the immunodetection of target proteins corresponding to Figure 1G.

(**D**) Comparative sequence analysis of the kinase domain between different animal species and human sequence showing a fully conserved peptide sequence between rodents, dogs and humans.

(**E**) *In vitro* dose response of PATAS peptide to trigger glucose uptake in mature adipocyte from different animal species and human mature adipocytes in absence of INS (n = 6-8 wells per condition).

Supplemental Figure S2.

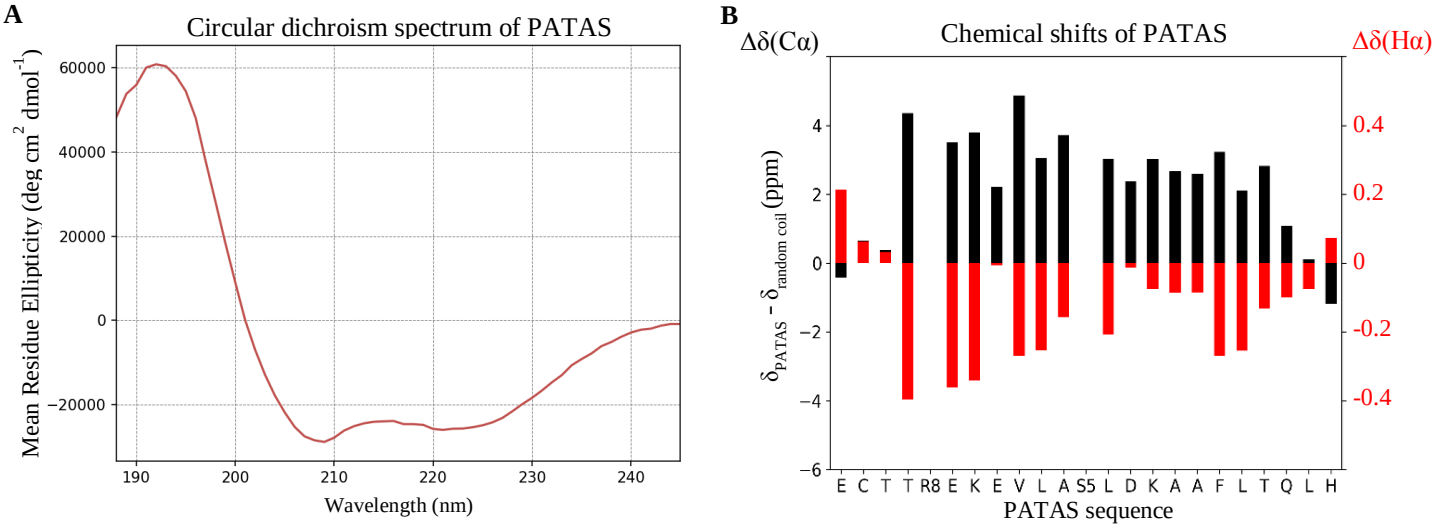

C

PKCα-ALMS1 PLA duolink

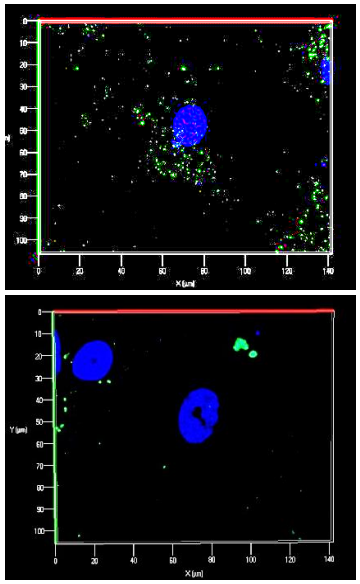

D

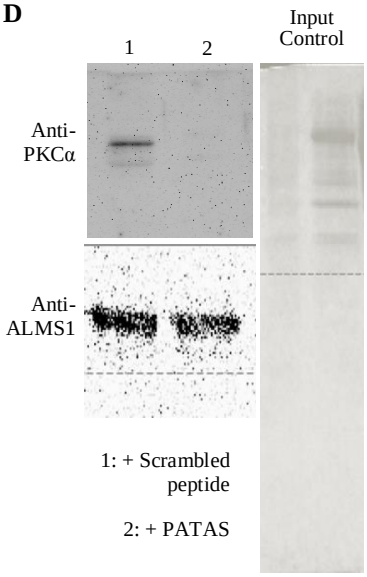

E

PATAS binding to ALMS1 in adipocyte

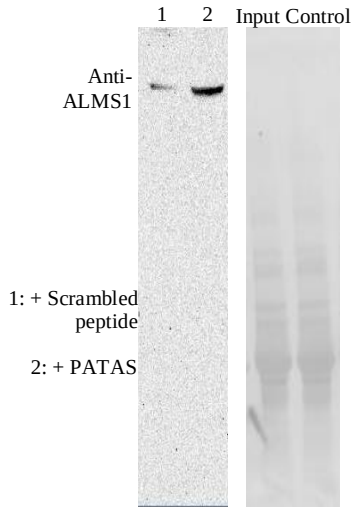

Peptide sequence used for PATAS antibody: ECTTVEKEVLALL

F

GLUT4 fusion with the PM upon PATAS treatment in human adipocyte

-INS

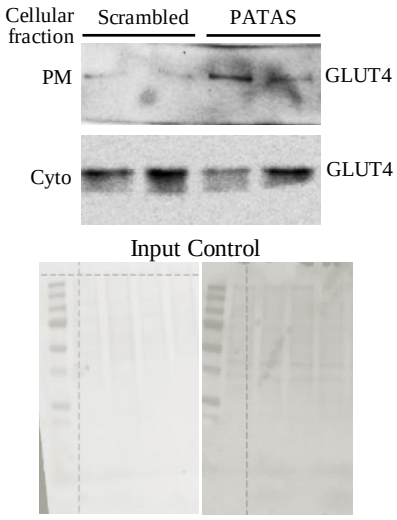

G

ipGTT in 6-month-old Alms foz/foz mice

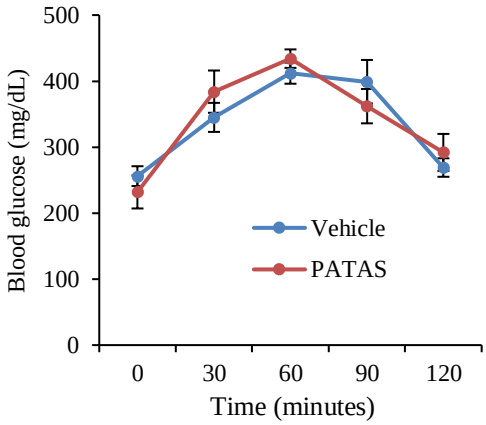

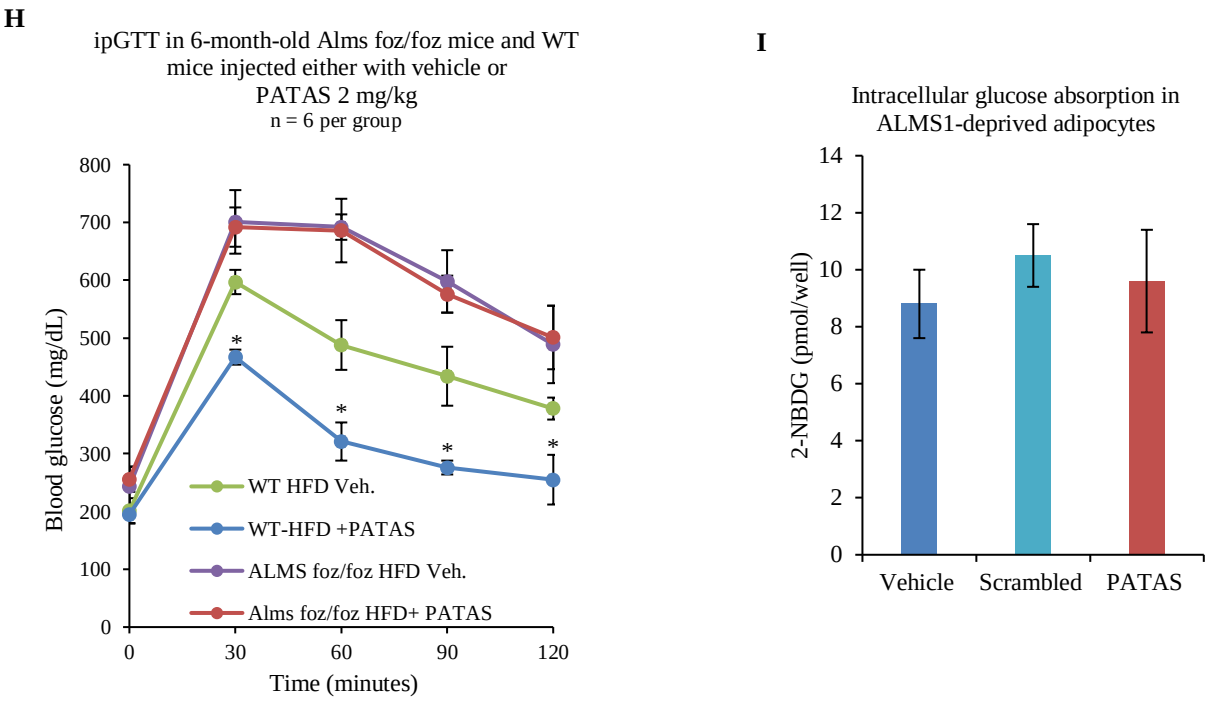

Figure S2. Characterizing PATAS cellular effects

(**A**) Far-UV circular dichroism spectrum of PATAS in a solution containing 75 % Methanol and 25 % saline aqueous solution (0.9 %) at 25°C.

(**B**) Comparison of Cα (in black) and Hα (in red) chemical shifts measured for PATAS peptide with random coil values from POTENCI software (4). Experimental chemical shifts were measured at 27°C after a complete resonance assignment was performed.

(**C**) PLA-Duolink analysis for ALMS1 and PKCα protein-protein interaction in presence of either a control scrambled peptide or PATAS peptide in absence of INS.

(**D**) Left panel: Immunodetection of PKCα and ALMS1 on immunoprecipitate of human adipocytes protein extracts using ALMS1 as bait in adipocytes cell lysates cultured in absence of INS and treated with either scrambled peptide or PATAS peptide. Right panel: loading control using Ponceau staining.

(**E**) Immunodetection of ALMS1 on immunoprecipitate of human adipocytes protein extracts using PATAS as the bait. An anti-PATAS mouse monoclonal was generated using the peptide sequence indicated. Right panel: loading control using Ponceau staining.

(**F**) Glut4 plasma membrane (PM) and cytosolic (Cyto) protein content from human adipocytes cultured in absence of insulin and treated with PATAS compared to scrambled peptide (up panel). Down panel depicts corresponding Ponceau stained membrane for loading controls.

(**G**) Blood glucose excursion curve during ipGTT on 6-month-old Alms1 foz/foz mice injected either with vehicle (in blue) or PATAS 2 mg/kg (in red) (n = 8 mice per group).

(**H**) Blood glucose excursion curve during ipGTT on 6-month-old Alms foz/foz mice and WT both fed with high fat diet (HFD) injected either with vehicle (in green and purple) or PATAS 2mg/kg (in blue and red). (n = 6 mice per group).

(**I**) Quantification of 2-NBDG cellular uptake in ALMS1-deprived human adipocytes following 30-minute incubation with either vehicle (in blue), scrambled peptide (in cyan) or PATAS (in red) (n = 8 wells per group).

Supplemental Figure S3.

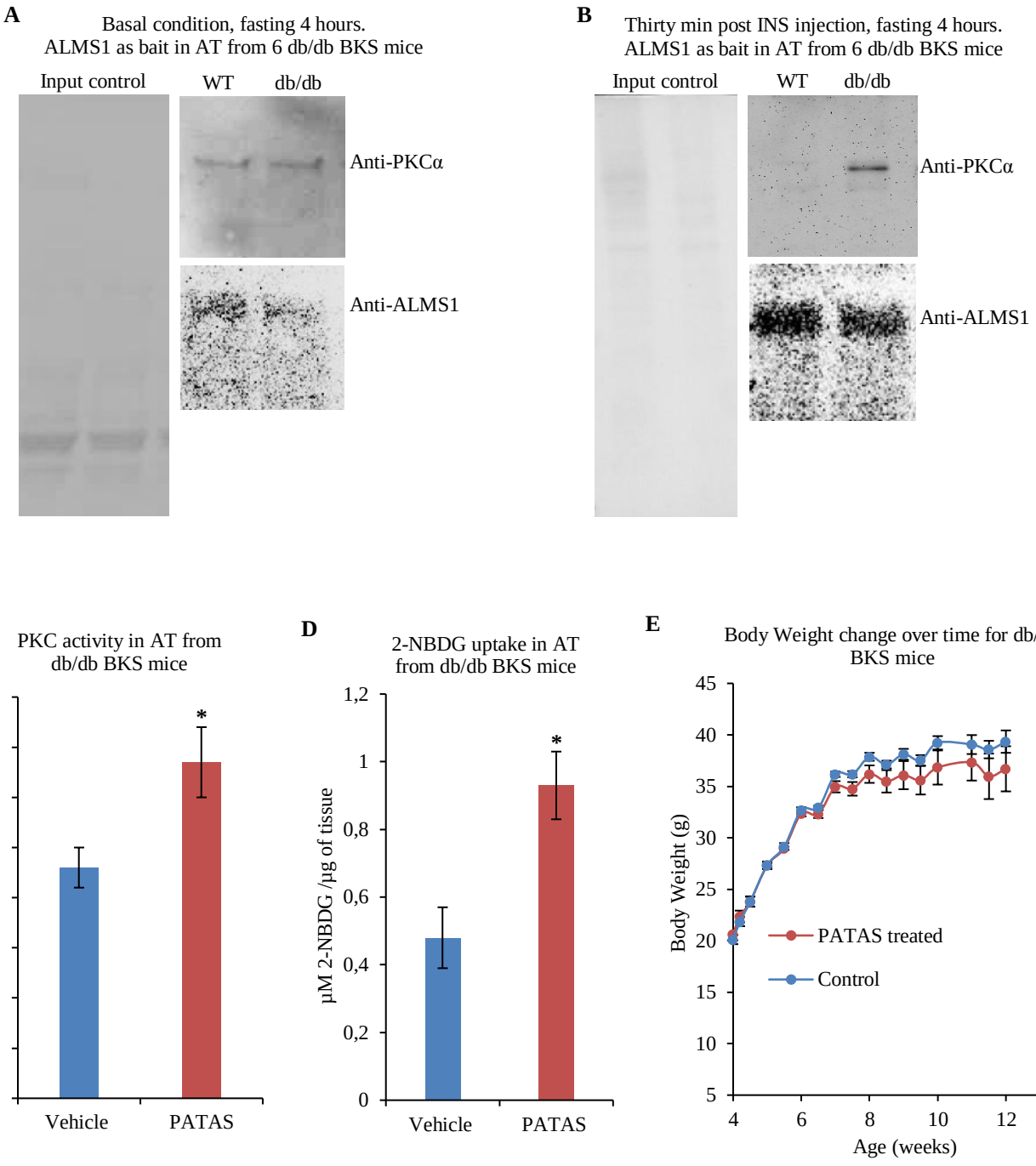

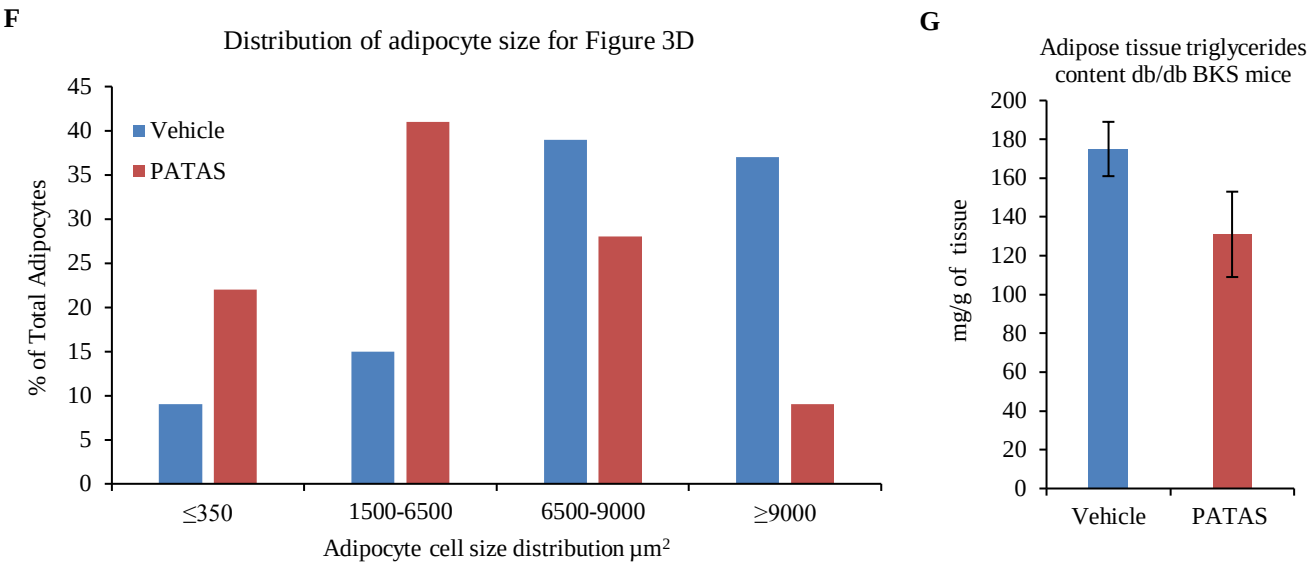

Figure S3. In-depth characterization of PATAS effect in db/db BKS mice

(**A**) Representative immunodetection of PKCα on AT protein extract immunoprecipitate from either 6-week-old WT or db/db BKS mice under 4 hours of fasting with ALMS1 as bait.

(**B**) Representative immunodetection of PKCα on AT protein extract immunoprecipitate from either 6-week-old WT or db/db BKS mice post 30 minutes insulin injection with ALMS1 as bait.

(**C**) Quantification of PKC activity in the AT following PATAS administration. Six-week-old db/db BKS mice received a subcutaneous injection of either saline as vehicle (in blue) or 2 mg/kg BW of PATAS solution (in red) and 30 minutes later the AT at the site of injection was harvested and processed to measure active PKC (n = 4 mice per group). * $p < 0.05$

(**D**) Quantification of glucose analogue (2-NBDG) uptake in the AT of db/db BKS mice 30 minutes post 2 mg/kg BW PATAS (in red) or vehicle (in blue) subcutaneous injection (n = 5 mice per group). * $p < 0.05$

(**E**) Body weight change over time for db/db BKS mice with a weekly injection of either 2 mg/kg BW PATAS (in red) or vehicle (in blue) starting at 8 weeks of age (n = 7 mice per group).

(**F**) Quantification of the adipocyte size distribution in PATAS-treated adipose tissue (in red) compared with vehicle-treated adipose tissue (in blue) corresponding to the representative pictures in Fig. 3D.

(**G**) Quantification of adipose tissue triglycerides content in PATAS-treated (in red) versus vehicle treated (in blue) db/db BKS mice after 4 weeks of weekly PATAS administration (n = 6 per group).

Supplemental Figure S4.

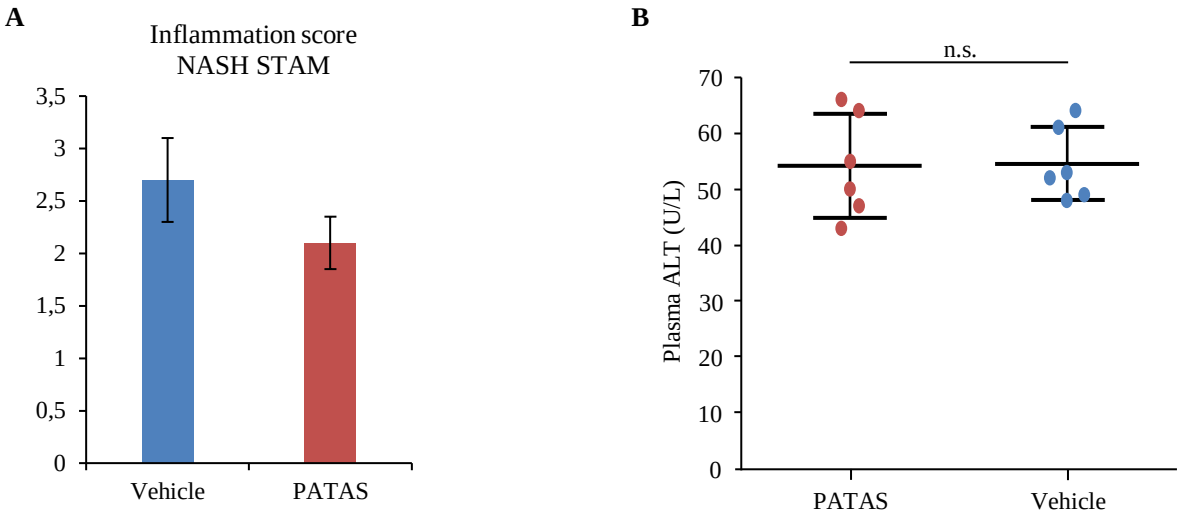

C

Data shown were normalized to the maximal and minimal response observed in the presence of control ligand and vehicle respectively (y-axis) and is plotted against the corresponding compound concentration in nM in log10 scale (x-axis).

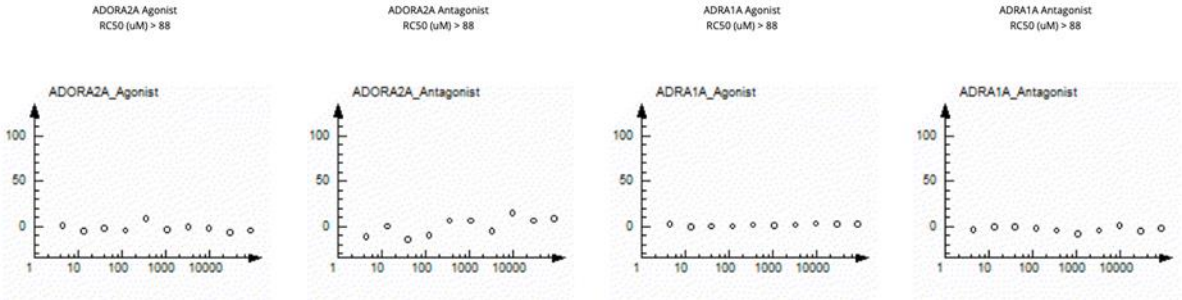

ADRA2A Agonist
RC50 (uM) > 88

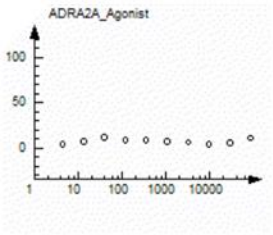

ADRA2A Antagonist
RC50 (uM) > 88

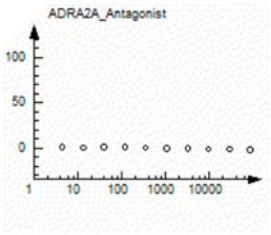

ADRB1 Agonist
RC50 (uM) > 88

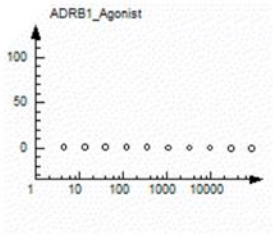

ADRB1 Antagonist
RC50 (uM) > 88

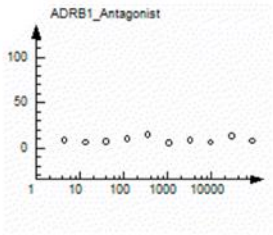

ADRB2 Agonist
RC50 (uM) > 88

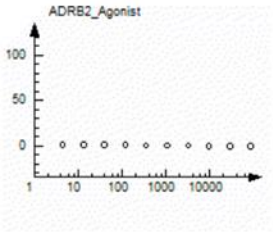

ADRB2 Antagonist
RC50 (uM) > 88

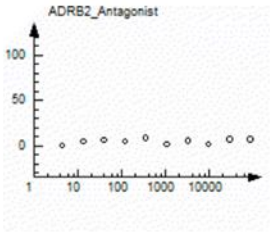

AVPR1A Agonist
RC50 (uM) > 88

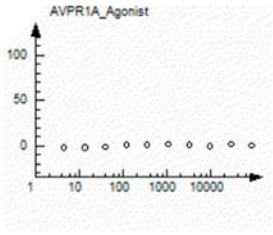

AVPR1A Antagonist
RC50 (uM) > 88

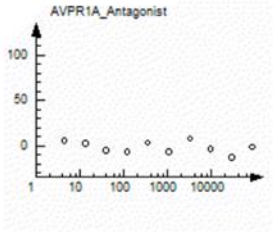

CCKAR Agonist
RC50 (uM) > 88

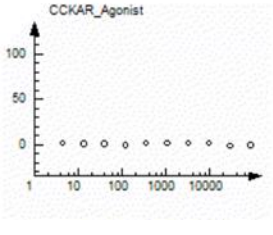

CCKAR Antagonist
RC50 (uM) > 88

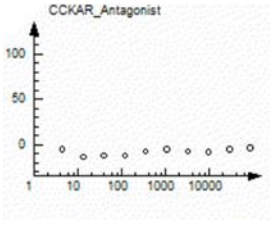

CHRM1 Agonist
RC50 (uM) > 88

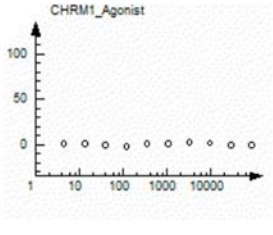

CHRM1 Antagonist
RC50 (uM) > 88

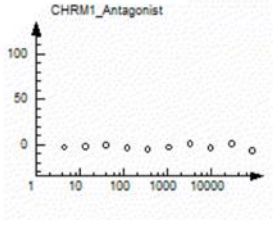

HTR1A Agonist
RC50 (uM) > 88

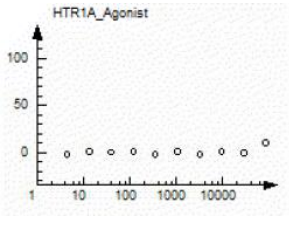

HTR1A Antagonist
RC50 (uM) > 88

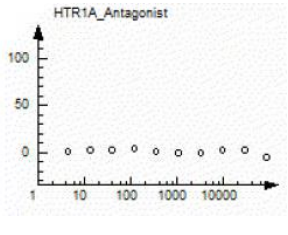

CNR1 Agonist
RC50 (uM) > 88

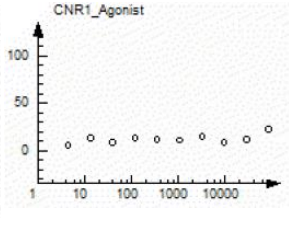

CNR1 Antagonist
RC50 (uM) > 88

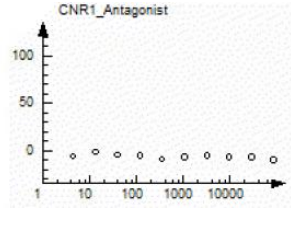

DRD1 Agonist
RC50 (uM) > 88

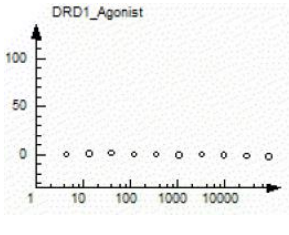

DRD1 Antagonist
RC50 (uM) > 88

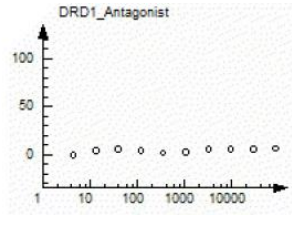

DRD2S Agonist
RC50 (uM) > 88

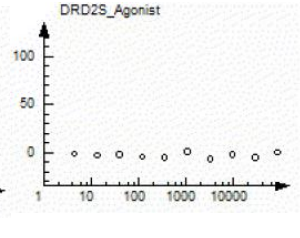

DRD2S Antagonist
RC50 (uM) > 88

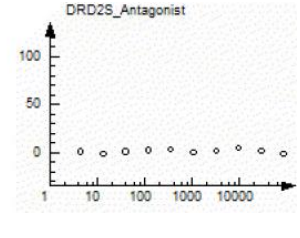

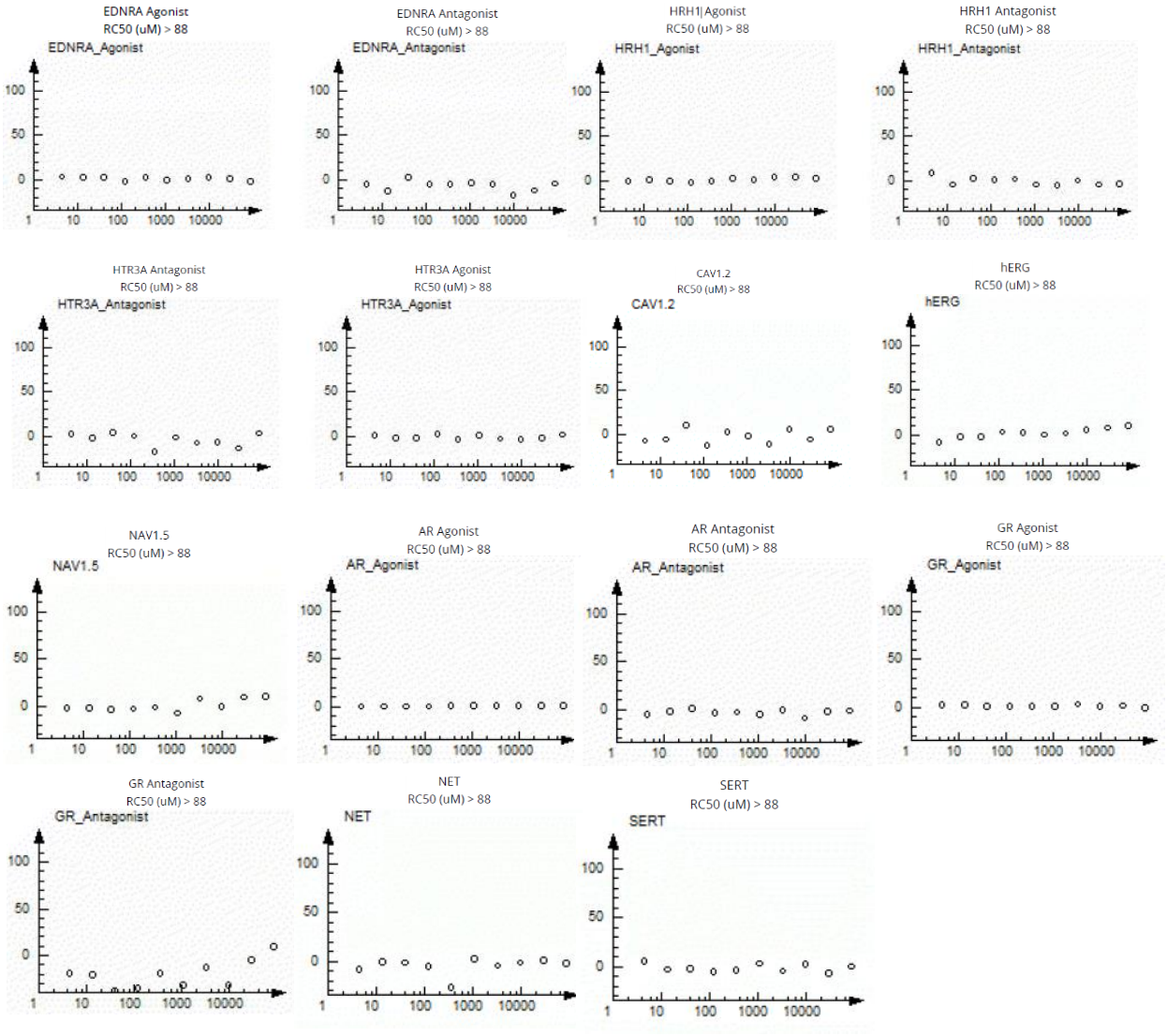

Figure S4. Effect of PATAS on NASH-STAM inflammation score and circulating ALT levels

(**A**) Quantification of hepatic inflammation score in NASH-STAM PATAS-treated group (in red) compared to vehicle-treated group (in blue) mice (n = 6 mice per group).

(**B**) Quantification of circulating ALT in NASH-STAM PATAS-treated group (in red) compared to vehicle-treated group (in blue) mice (n = 6 mice per group).

(**C**) Selected data set from the DiscoverX SAFETYscan™ E/IC50 screen for PATAS depicting the absence of activity on the 22 tested targets on the assay.

Supplemental Figure S5.

A

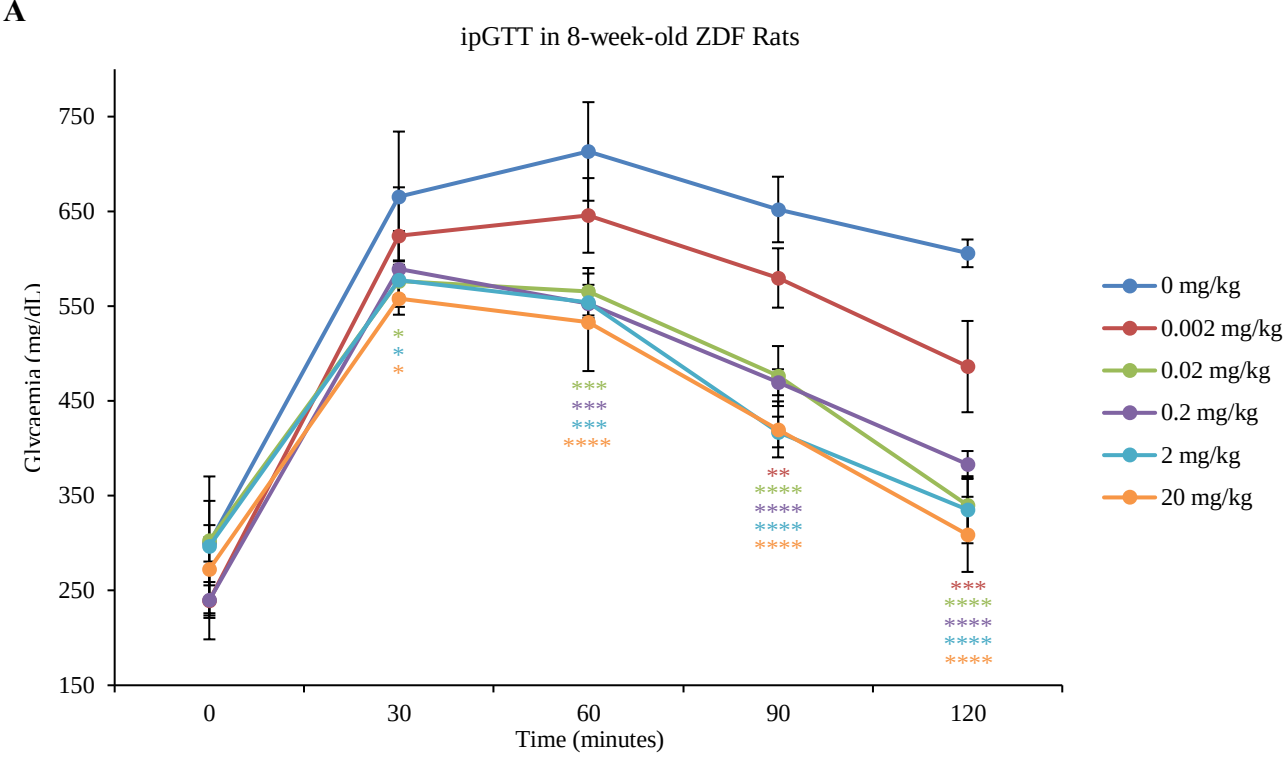

B

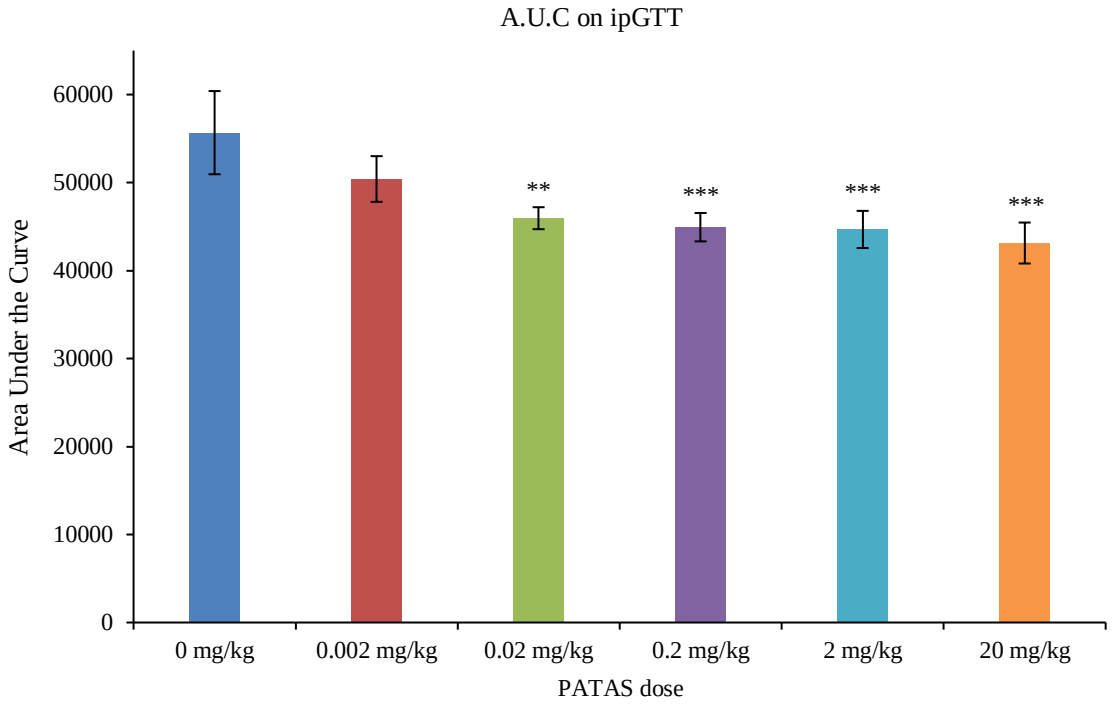

Figure S5. *In vivo* dose response of PATAS on ipGTT in diabetic Zucker rats

(**A**) Blood glucose excursion curve during ipGTT 4 days after PATAS subcutaneous injection at increasing doses, following a 16-hour fasting period (n = 4 rats per group). * $p < 0.05$, ** $p < 0.01$, *** $p < 0.001$, **** $p < 0.0001$

(**B**) Corresponding Area Under the Curve (AUC) of (**A**). ** $p < 0.01$, *** $p < 0.001$

Supplemental Figure S6.

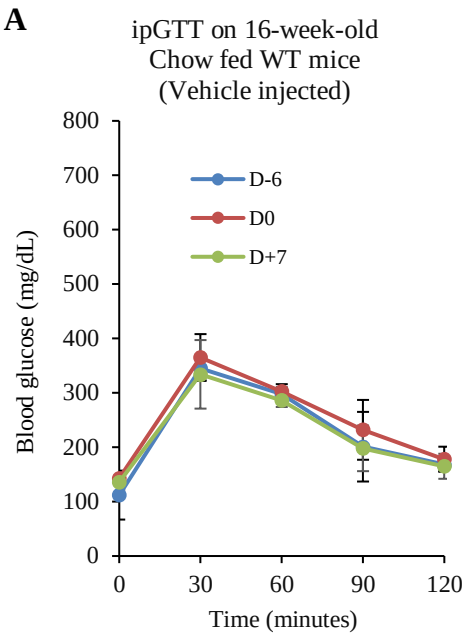

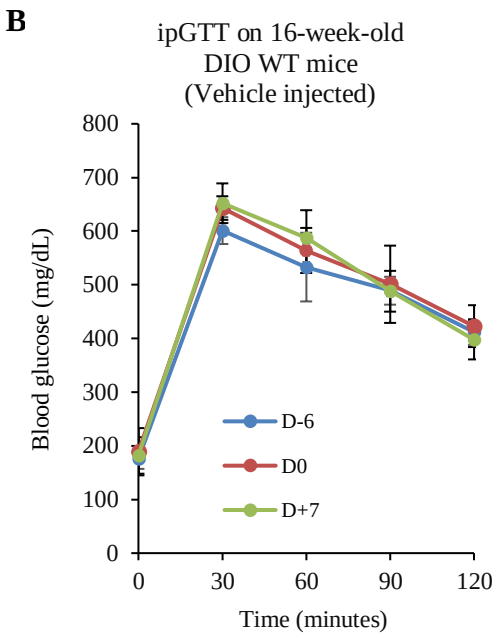

C

PATAS pharmacokinetic parameters in mice

Test Article	Dose Route	Dose Level (µg/animal)	Dose Conc. (mg/mL)	$T_{1/2}$ (hr)	Cl (mL/hr/kg)
Mouse serum	Subcutaneous adipose tissue	100	2.5	4.32	357

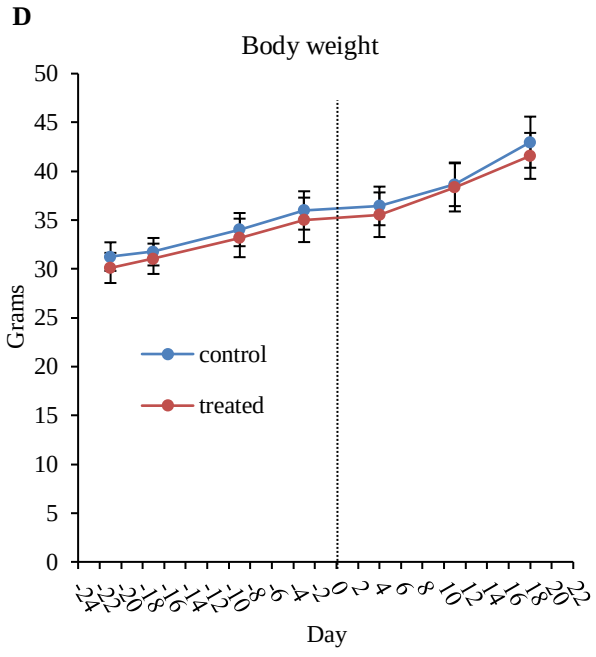

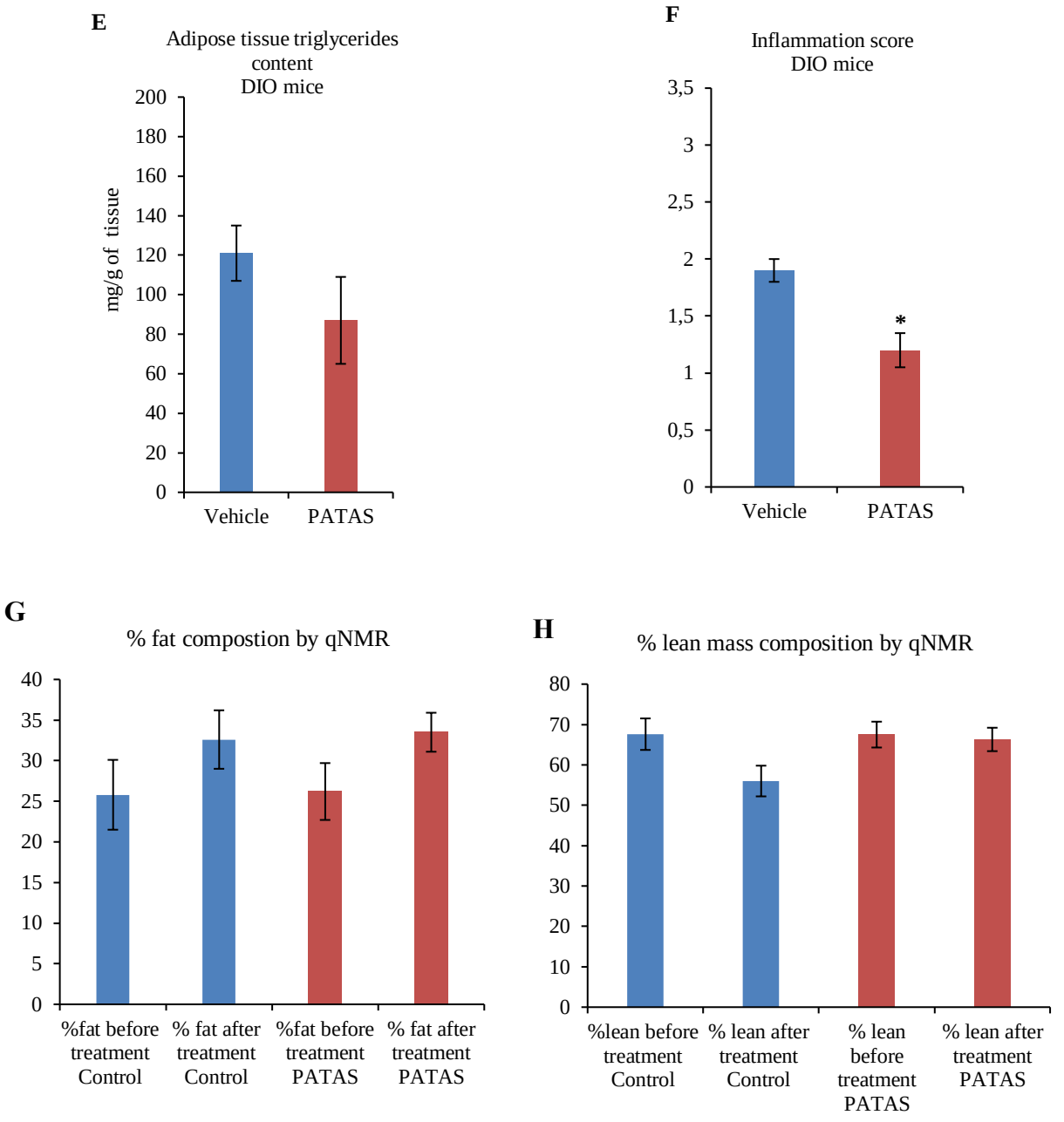

Figure S6. Effect of PATAS on Body mass composition determined by quantitative NMR in DIO WT mice

(**A**) Blood glucose excursion curve during ipGTT 6 days before Vehicle injection (D-6, in blue), on the day of Vehicle injection (D0, in red) and 7 days post Vehicle injection (D+7, in green) on the same chow-fed mice. (n = 6 mice).

(**B**) Blood glucose excursion curve during ipGTT 6 days before Vehicle injection (D-6, in blue), on the day of Vehicle injection (D0, in red) and 7 days post Vehicle injection (D+7, in green) on the same high fat/high glucose fed, diet-induced obese (DIO) mice. (n = 6 mice).

(**C**) PATAS pharmacokinetic parameters in mice: $T_{1/2}$ for terminal half-life, Cl for total body (n = 24 mice per group).

(**D**) Body weight change over time before initiation of PATAS treatment (from -24 to Day 0) then during the PATAS treatment period (from D1 to D22) with a weekly 2 mg/kg BW PATAS injection (in red) versus saline solution control (in blue).

Age of mice at D-24: 16 weeks.

(**E**) Quantification of adipose tissue triglycerides content in PATAS-treated (in red) versus vehicle treated (in blue) DIO mice after 4 weeks of weekly PATAS administration (n = 6 per group).

(**F**) Quantification of hepatic inflammation score in DIO PATAS-treated group (in red) compared to vehicle-treated group (in blue) mice (n = 6 mice per group). * $p < 0.05$

(**G**) Percentage fat composition for PATAS (in red) and control (in blue) groups before (D-7) and after treatment (D+20).

(**H**) Corresponding percentage lean mass composition for PATAS (in red) and control (in blue) groups before (D-7) and after treatment (D+20) (n = 10 mice per group).

SUPPLEMENTAL REFERENCES

1. K. A. Carswell, M.-J. Lee, S. K. Fried, Culture of isolated human adipocytes and isolated adipose tissue. *Methods Mol Biol* **806**, 203–214 (2012).
2. D. E. Kleiner, *et al.*, Design and validation of a histological scoring system for nonalcoholic fatty liver disease. *Hepatology* **41**, 1313–1321 (2005).
3. R. K. Singh, *et al.*, Protein kinase C-α and the regulation of diverse cell responses. *Biomol Concepts* **8**, 143–153 (2017).
4. J. T. Nielsen, F. A. A. Mulder, POTENCI: prediction of temperature, neighbor and pH-corrected chemical shifts for intrinsically disordered proteins. *J Biomol NMR* **70**, 141–165 (2018).